Current Instabilities in Resonant Tunneling Quantum Dot Structures

Kathy Lüdge and Eckehard Schöll
Technische Universität Berlin, Institut für Theoretische Physik

Introduction

The current transport through devices consisting of layers with quantum dots has attracted considerable interest for the semiconductor technology.

With decreasing dot size single electron/hole tunneling effects become visible leading to **single peaks** in the **I(V)** characteristic.

In the following the **current instabilities** in a resonant tunneling **Quantum Dot Structure** will be studied with a master equation approach. The structure is embedded in an **external circuit**. Due to the strong negative differential conductance several fixed points exist and the performance of the device is crucially dependent on the chosen parameters.

The **bifurcation analysis** is done using linear stability analysis for the QD system.

A **global bifurcation** is found with numerical integration.

Model of the QD System

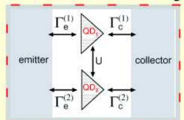

- QD system: two Quantum dots embedded between an emitter and a collector contact
- each QD has one discrete energy level ε_i
- U ... Xoulomb charging energy
- $\Gamma_{e/c}^{(i)}$ ... electron transition rate
- $f_e^{(i)}$ ... Fermi function at the emitter contact

Configuration Space (QD_1,QD_2)

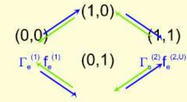

Master Equation

$$\dot{\underline{P}} = \underline{\underline{M}}\,\underline{P} \quad \text{with} \quad \underline{P} = (P_{00}, P_{10}, P_{01}, P_{11})^T$$

- master equation describes the temporal evolution of the occupation probabilities P_ν combined to the vector $\underline{P}$
- matrix M contains all gain and loss processes scetched above

$$\underline{\underline{M}} = \begin{pmatrix} -\Gamma_e^{(1)} f_e^{(1)} - \Gamma_e^{(2)} f_e^{(2)} & \Gamma_e^{(1)}(1-f_e^{(1)}) + \Gamma_c^{(1)} & \Gamma_e^{(2)}(1-f_e^{(2)}) + \Gamma_c^{(2)} & 0 \\ \Gamma_e^{(1)} f_e^{(1)} & -\Gamma_e^{(1)}(1-f_e^{(1)}) - \Gamma_c^{(1)} - \Gamma_e^{(2)} f_e^{(2,U)} & 0 & \Gamma_e^{(2)}(1-f_e^{(2,U)}) + \Gamma_c^{(2)} \\ \Gamma_e^{(2)} f_e^{(2)} & 0 & -\Gamma_e^{(1)} f_e^{(1,U)} - \Gamma_e^{(2)}(1-f_e^{(2)}) - \Gamma_c^{(2)} & \Gamma_e^{(1)}(1-f_e^{(1,U)}) + \Gamma_c^{(1)} \\ 0 & \Gamma_e^{(2)} f_e^{(2,U)} & \Gamma_e^{(1)} f_e^{(1,U)} & \Gamma_e^{(1)} f_e^{(1,U)} + \Gamma_e^{(2)} f_e^{(2,U)} - \Gamma \end{pmatrix}$$

with $\epsilon_1 = \epsilon_2$, $\Gamma_e^{(1)} = \Gamma_c^{(1)} = \Gamma_e^{(2)}$, $\Gamma_c^{(2)} = 0.01 \cdot \Gamma_e^{(2)}$, $U = k_B T/0.03 \approx 2.87 meV$

Electronic Circuit

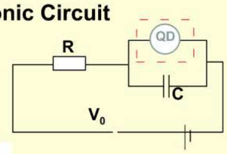

- external circuit ensures a **global coupling**
- additional dynamic variable **U**
- capacity C and resistance R are easily changeable parameters

Dynamics of the System (I-V) will be analysed for different parameters R and C.

Differential equations

$$\text{(I-IV)} \quad \frac{d}{dt}\underline{P} = \underline{\underline{M}}(V)\underline{P}$$

$$\text{(V)} \quad C\frac{d}{dt}V = \frac{V_0 - V}{R} - \langle I(\underline{P}, V)\rangle$$

$$\langle I \rangle = \frac{1}{2}\sum_\nu \left[\underline{\underline{j}}_c \underline{P} + \underline{\underline{j}}_e \underline{P}\right]_\nu$$

Current propagator

Collector

$$\underline{\underline{j}}_c = e \begin{pmatrix} 0 & \Gamma_c^{(1)} & \Gamma_c^{(2)} & 0 \\ 0 & 0 & 0 & \Gamma_c^{(2)} \\ 0 & 0 & 0 & \Gamma_c^{(1)} \\ 0 & 0 & 0 & 0 \end{pmatrix}$$

Emitter

$$\underline{\underline{j}}_e = e \begin{pmatrix} 0 & -\Gamma_e^{(1)}(1-f_e^{(1)}) & -\Gamma_e^{(2)}(1-f_e^{(2)}) & 0 \\ \Gamma_e^{(2)} f_e^{(2)} & 0 & 0 & -\Gamma_e^{(1)}(1-f_e^{(1,U)}) \\ \Gamma_e^{(1)} f_e^{(1)} & 0 & 0 & -\Gamma_e^{(2)}(1-f_e^{(2,U)}) \\ 0 & \Gamma_e^{(1)} f_e^{(1,U)} & \Gamma_e^{(2)} f_e^{(2,U)} & 0 \end{pmatrix}$$

Resistance R

Passive external circuit (R,C positive)

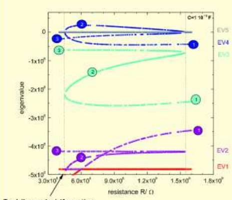

- for a passive external circuit **two** stable nodes and **one** saddle point exist in phase space
- the saddle point separates the basins of attraction for the two stable nodes
- all eigenvalues are real
- a Hopf bifurcation is NOT possible because the analytic condition cannot be fullfiled
- where the load line touches the extrema of the stationary current Saddle node bifurcations occure

Possible Applications

- fast **switching** of the device could be achieved by either varying the external voltage V_0 or the series resistance R

Active External circuit (C negative)

Bifurcation diagram

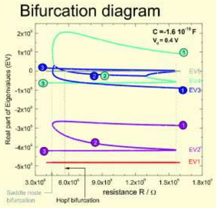

- for an active external circuit the two fixed points on the positive conductivity branches 1 & 3 are saddle points while the fixpoint in the middle 2 undergoes a **Hopf bifurcation**
- eigenvalues are real exept two eigenvalues of the middle branch 2
- Saddle node bifurcations at $R=4.55\,10^8\,\Omega$ and $R=1.56\,10^9\,\Omega$

Stationary solutions

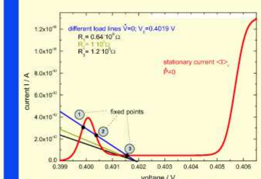

- relaxation time of the circuit RC is chose to be of the order of the transition rates $1/\Gamma$
- three fixed points for $V_0 \sim 0.4019$ V and $R= 4\,10^8 ... 1.6\,10^9\,\Omega$

Capacitance C

Bifurcation diagram at fixed point 2

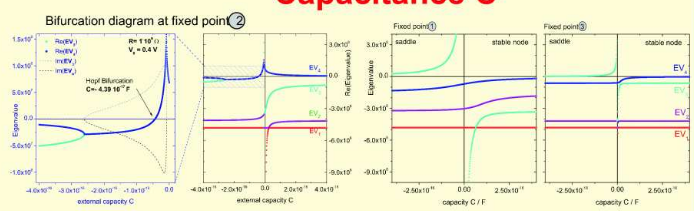

- with negative C the fixpoint on branch 2 undergoes a Hopf Bifurcation
- there is no inverse Hopf bifurcation which ensures a shrinking Limit Cycle - Instead the LC collides with the saddle ponit in a Blue Sky Catastroph
- the fixpoints on the positive conductivity branches are saddle points or stable nodes depending on the polarity of C
- negative capacitance, can easily be realized by an active circuit consisting of operation amplifiers [2,3]

Blue Sky Catastrophe-Global Bifurcation

Transients in Phase Space

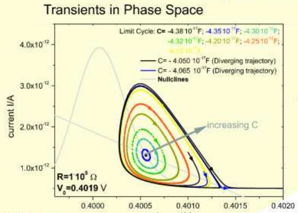

Frequency at the bifurcation Point

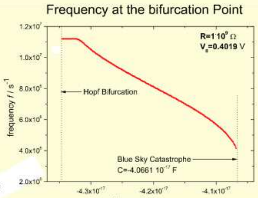

- the frequency stays constant at the Hopf bifurcation while it goes to zero (infinite period) at the global homoclinic bifurcation
- after the LC has touched the saddle point (blue sky catastrophe) there is no stable fixed point in the system

Bifurcation diagram in R-C Space

Fixed Point 2

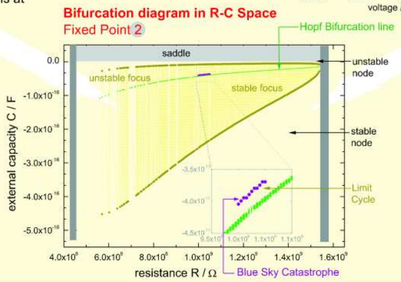

- following the Hopf bifurcation through the parameter space (R,C) one obtains the green line that shows the transition from the stable focus to the LC and an unstable focus
- in the shaded areas the eigenvalues are all real
- the limit cycle vanishes at the homoclinic bifurcation which is exemplary shown for R appr. $1\,10^9\,\Omega$ with the violet dots

References

[1] Kießlich, G., Wacker, A. and Schöll, Physica B 314, 459-463 (2002)
[2] National Semiconductor Application Note 31, February 1978, Op Amp Circuit Collection
[3] Martin A. D., Lerch M. L. F., Simmonds P. E., and Eaves L., Appl. Phys. Lett. 64, 1248 (1994)
[4] Schöll, E., Amann, A., Rudolf, M. and Unkelbach, Physica B 314, 113-117 (2002)

Comparison to double barrier resonant tunneling diode with quantum well

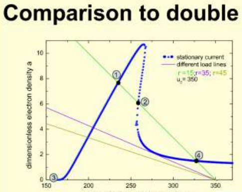

$$u = \frac{eU}{kT} \qquad a = \frac{n}{\rho_0 kT}$$

- Stationary solutions show a Z-shaped I(V) curve

Stability: eigenvalues

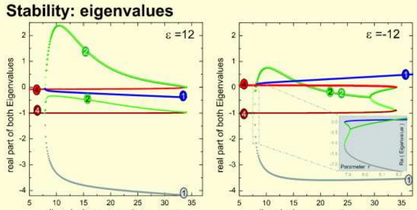

- Parameter:

$$r = \frac{Rc^2 \rho_0 L_x L_y}{\tau_a} \qquad \varepsilon = \frac{RC}{\tau_a}$$

- Comparing the performance of both systems some similarities but also some essential differences can be found. The Z-shape of the DBRT I(V) curve has a bistability range leading to a inverse Hopf bifurcation. This ensures the existence of at least one stable fixed point.

Summary

For C>0 we show that oscillatory instabilities caused by a Hopf bifurcation cannot occure. There is a saddle-point on the negative conductivity branch that **separates the basins of attraction** for the two stable nodes.

Thus, the resonant tunneling QD structure could be used as a fast switching device

For C<0 a there is a Hopf bifurcation leading to uniform limit cycle oscillations. With increasing absolute value of C the oscillation amplitude increases while its shape transforms from an elliptic to a strongly nonlinear relaxation-type shape. At a certain value of C the limit cycle collides with the saddle-point on the low current branch and disappears. This represents a global homoclinic bifurcation.

Comparing the performance with a conventional double barrier resonant tunneling diode (DBRT) using a quantum well [4] we find that for the N-shape of the QD I(V) no inverse Hopf bifurcation exists but parameter sets whithout stable fixed points.

Acknowledgement

This work was supported by Sfb 555.